College of Natural and Applied Sciences

10-1-2011

Period and amplitude variability of the high-amplitude δ Scuti star gp andromedae

A.-Y. Zhou
Missouri State University

S. Y. Jiang

PERIOD AND AMPLITUDE VARIABILITY OF THE HIGH-AMPLITUDE δ SCUTI STAR GP ANDROMEDAE

A.-Y. ZHOU[1] AND S.-Y. JIANG

National Astronomical Observatories, Chinese Academy of Sciences, 20A Datun Road,
100012 Beijing, China; aiying@nao.cas.cn

ABSTRACT

Extensive differential time-series CCD photometry has been carried out between 2003 and 2009 for the high-amplitude δ Scuti (HADS) star GP And. We acquired 12,583 new measurements consisting of 41 nights (153.3 hr) spanning over 2221 days. This is the largest time-series data set to date for the star. Based upon these data and others available in the literature, a comprehensive analysis has been conducted to investigate the pulsational properties of the star. Except for the known fundamental period and its harmonics we failed to detect any additional pulsation periods either radial or nonradial. We show clear amplitude variability, but we failed to verify the previously claimed periodic amplitude modulation. Classic $O-C$ analysis indicates that the fundamental pulsation period of GP And is slowly increasing at a rate of $\dot{P}/P = (5.49 \pm 0.1) \times 10^{-8}$ yr^{-1} in accordance with the predictions of stellar evolutionary models. Findings of nonradial oscillations in previously known radial high-amplitude pulsators are being increasingly reported. We have briefly reviewed the current status of multiperiodicity and nonradial pulsation features among the high-amplitude pulsators in the classic instability strip.

Key words: stars: individual (GP And) – stars: oscillations – stars: variables: delta Scuti

Online-only material: color figures

1. INTRODUCTION

GP Andromedae (= HIP 4322 = GSC 01739–01526, $\langle V \rangle \sim 10\overset{m}{.}7$, $\Delta V \sim 0\overset{m}{.}55$, $P_0 = 0\overset{d}{.}0787$, A3) is a Population I high-amplitude δ Scuti star of fundamental mode pulsation (Breger & Pamyatnykh 1998; Rodríguez et al. 2000). δ Sct stars are short-period ($\lesssim 0.3$ day) pulsators situated inside the lower part of the classical Cepheid instability strip on and near the main sequence (MS), with spectral types ranging from about A2 to F6. The high-amplitude δ Sct stars (HADS, $\Delta V \geqslant 0\overset{m}{.}3$) constitute a subgroup of δ Sct stars. Statistics of the Rodríguez et al. (2000) catalog show that about a quarter of δ Sct stars (155 from 636) are HADS. They have exceptionally low rotational velocities of $v \sin i \leqslant 30$ km s^{-1} with pulsation properties resembling the classic Cepheids and RR Lyrae stars. HADS appear to have only one or two radial pulsation modes, in the fundamental and/or first overtone mode. As such, stars in the HADS subgroup were historically referred to as dwarf Cepheids, AI Vel stars, or RR stars in early literature.

A predicted period change (increase) due to stellar evolution exists for stars of δ Sct-type in the lower instability strip. Since the period is related to the structure of the star through the pulsation equation $P\sqrt{\rho} = Q$, the period change is therefore related to the radius change, if we assume that the star's mass does not vary. As a consequence, one may hope that the small changes in pulsation period have the potential to help reveal evolutionary changes in the stellar structure (Breger & Pamyatnykh 1998). Two recent studies for GP And (Szeidl et al. 2006; Pop et al. 2003) show increasing pulsational period changes with a rate of $\dot{P}/P \sim 6 \times 10^{-8}$ yr^{-1}. In addition, Rodríguez et al. (1993) derived its stellar physical parameters, which suggest a late MS evolutionary stage with an age over 1 Gyr.

GP And has a faint visual companion star GSC 01739–01964 ($\alpha_{2000} = 00^h 55^m 18\overset{s}{.}83$, $\delta_{2000} = +23°09'45\overset{''}{.}94$, $V = 12\overset{m}{.}5$) separated by 10.99 arcsec (Tycho-2 catalog; Eggen 1978; Morlet et al. 2000). The quoted right ascension and declination values are determined by the author from the POSS1 Blue images of the STScI Digitized Sky Survey. Most published photometry of GP And contains this faint star and observations were largely conducted to measure times of maximum light. In order to study a possible disturbance or modulation in the light variation like that claimed by Gieseking et al. (1979), we needed to acquire an extensive time-series data set. Such a data set is also useful to examine any dependence of the star's pulsational behavior on the faint companion.

Encouraged by these ideas, we have collected what is currently the longest set of time-series CCD photometric data for GP And between 2003 and 2009. With these new data, together with those available in the literature, we are now able to resolve possible closely spaced pulsations of the star in a higher frequency resolution.[2] We can measure period changes as well as examine amplitude variability on a longer time baseline. Following a data description in Section 2, analyses of the data and the results are presented in Section 3. Discussions of the results and our conclusions are given in the last two sections.

2. OBSERVATIONS AND DATA REDUCTION

CCD photometry of GP And was performed between 2003 and 2009 using several different CCD cameras on three telescopes. In 2003, 2006, 2007, 2008, and 2009, observations were made with either an Apogee AP7P CCD camera 512×512 in size or a Princeton Instruments MicroMAX:1024BFT CCD (MiCPhot; Zhou et al. 2009) mounted on the 85 cm telescope at

---

[2] Frequency resolution is the minimum difference in frequency between two sinusoids which allows two distinct peaks to be resolved in the spectrum. We usually take the Rayleigh frequency limit defined to be the inverse of the time interval of a series of measurements or the sampling rate divided by the number of samples.

Table 1
Observing Log of CCD Photometry of GP And

Date (UT)	Duration	Frames	Maxima	Δt	Instrument
2003.11.08	2951.964–2952.178	620	2	20	AP7P, 85cm, BAO
2004.09.22	3270.922–3270.974	215	1	20	Alta U47+, 40cm, Baker
2004.09.26	3274.922–3274.979	236	0	20	Alta U47+, 40cm, Baker
2004.09.27	3275.919–3275.981	256	1	20	Alta U47+, 40cm, Baker
2004.09.30	3278.911–3278.984	300	1	20	PI RS1340b, 40cm, Baker
2004.10.03	3281.872–3281.935	262	1	20	PI RS1340b, 40cm, Baker
2006.08.26	3974.247–3974.364	155	1	40	AP7P, 85cm, BAO
2006.08.31	3979.234–3979.366	230	2	40	AP7P, 85cm, BAO
2006.09.05	3984.239–3984.370	224	1	40	AP7P, 85cm, BAO
2006.09.06	3985.210–3985.328	174	1	40	AP7P, 85cm, BAO
2006.09.08	3987.192–3987.381	329	3	40	AP7P, 85cm, BAO
2006.09.09	3988.314–3988.372	123	1	30	AP7P, 85cm, BAO
2006.09.10	3989.208–3989.372	360	2	30	AP7P, 85cm, BAO
2006.09.11	3990.192–3990.255	155	2	30	AP7P, 85cm, BAO
2006.10.03	4012.306–4012.382	133	1	40	AP7P, 85cm, BAO
2006.10.04	4013.136–4013.363	441	3	40	AP7P, 85cm, BAO
2006.10.05	4013.980–4014.174	338	2	40	AP7P, 85cm, BAO
2006.10.09	4017.976–4018.340	468	5	60	AP7P, 85cm, BAO
2006.10.25	4034.009–4034.046	29	1	60	AP7P, 85cm, BAO
2006.10.26	4034.934–4035.157	157	3	60	AP7P, 85cm, BAO
2006.10.28	4036.929–4037.119	232	3	60	AP7P, 85cm, BAO
2006.10.29	4037.930–4038.119	157	2	60	AP7P, 85cm, BAO
2006.10.30	4038.927–4038.957	27	0	60	AP7P, 85cm, BAO
2006.10.31	4039.939–4040.130	215	1	60	AP7P, 85cm, BAO
2006.11.01	4040.953–4041.147	283	3	60	AP7P, 85cm, BAO
2006.11.02	4041.930–4042.126	341	2	40	AP7P, 85cm, BAO
2006.11.04	4043.927–4044.122	337	3	40	AP7P, 85cm, BAO
2006.11.05	4044.928–4045.219	503	4	40	AP7P, 85cm, BAO
2006.11.06	4045.924–4046.191	230	3	90	AP7P, 85cm, BAO
2007.12.01	4435.982–4436.192	3755	3	6	MiCPhot, 85cm, BAO
2007.12.02	4436.909–4437.171	4893	3	5	MiCPhot, 85cm, BAO
2007.12.03	4437.917–4438.176	4041	3	5	MiCPhot, 85cm, BAO
2007.12.04	4438.939–4439.220	2795	2	6	MiCPhot, 85cm, BAO
2007.12.06	4440.932–4441.177	2070	3	6	MiCPhot, 85cm, BAO
2008.01.29	4494.292–4494.376	75	1	90	BFOSC, 2.16m, BAO
2008.01.30	4495.286–4495.368	83	1	90	BFOSC, 2.16m, BAO
2008.01.31	4496.314–4496.360	43	1	90	BFOSC, 2.16m, BAO
2008.08.02	4681.261–4681.353	359	1	10	MiCPhot, 85cm, BAO
2009.12.01	5166.982–5167.040	300	0	10	MiCPhot, 85cm, BAO
2009.12.06	5171.939–5172.233	1566	4	7	MiCPhot, 85cm, BAO
2009.12.07	5173.074–5173.202	880	1	10	MiCPhot, 85cm, BAO

Notes. Duration is given as HJD 2450000+, Δt is the exposure time of each frame in seconds. The "instrument" column gives CCD cameras or systems, telescopes, and observatories.

the Xinglong Station of the National Astronomical Observatories of the Chinese Academy of Sciences. A few data were obtained in 2008 by using the BFOSC system on the 2.16 m telescope (Huang et al. 2005). In 2004, either a Princeton Instruments RS1340b CCD camera or an Apogee Alta U47+ 1024×1024 CCD was used on the 40 cm telescope at the Baker Observatory of Missouri State University. The images from the 40 cm telescope were binned in 2 × 2 pixels.

Images were reduced with IRAF. The procedures of image reduction including bias and dark subtraction and flat-field correction, as well as the aperture-optimized photometry are the same as that outlined in Zhou et al. (2006). The photometry aperture may vary from frame to frame as it is optimized based on the full width at half-maximum determined via three well-exposed stars for each image. The reference stars observed in the field of GP And were detected as non-variables within the general observational error of about 0.005 minutes, a derived typical accuracy representing the standard deviation of the differential magnitudes between any two reference stars. The

photometry program measures each star on six apertures and builds differential magnitudes of the target relative to different numbers of reference stars. Then we performed differential photometry for GP And—one or multiple reference stars (up to five) were used as comparisons. Which aperture and how many reference stars are finally chosen depends on which set of resulting differential magnitudes are the best (which have the least scatter).

All observations throughout the six years (2003, 2004, 2006, 2007, 2008, and 2009) were obtained through a standard Johnson V or Johnson–Cousin–Bessel formula V filter. Exposure times varied from run to run depending on seeing conditions and different instrument systems. To improve data quality, observations exposed less than 30 s are binned to be 30 s or 60 s integrations per point. Finally, we obtained a total of 12,583 time-series measurements consisting of 41 nights (153.3 hr) spanning over 2221 days. A journal of the observations is given in Table 1. With these data we have detected a total of 78 new times of maximum light following the method illustrated

Table 2
New Times of Maximum Light of GP And Collected in 2003–2010

HJD$_{max}$	HJD$_{max}$	HJD$_{max}$
2442709.61860[a]	2454018.21873	2454436.96914
2442711.66220	2454018.29843	2454437.04760
2452951.98822	2454034.03386	2454437.12589
2452952.06694	2454034.97861	2454437.99176
2452952.14576	2454035.05597	2454438.07045
2453270.96846	2454035.13617	2454438.14913
2453275.92547	2454036.94560	2454439.09331
2453278.91525	2454037.02406	2454439.17197
2453281.90546	2454037.10293	2454440.98217
2453974.31383	2454037.96882	2454441.05992
2453979.27136	2454038.04803	2454441.13968
2453979.34898	2454040.09359	2454494.37086
2453984.30696	2454040.95881	2454495.31457
2453985.25171	2454041.03713	2454496.33803
2453987.21801	2454041.11579	2454681.27946
2453987.29696	2454041.98165	2454713.4600(7)
2453987.37610	2454042.06028	2454827.2354(6)
2453988.32015	2454043.94860	2454827.3142(6)
2453989.26430	2454044.02770	2454827.3929(6)
2453989.34237	2454044.10593	2454827.4716(6)
2453990.20872	2454044.97171	2455155.3448(7)
2454012.31833	2454045.05043	2455155.5017(9)
2454013.18353	2454045.12858	2455171.94552
2454013.26202	2454045.20789	2455172.02414
2454013.34077	2454045.99444	2455172.10275
2454014.04837	2454046.07317	2455172.18202
2454014.12708	2454046.15132	2455172.3392(9)
2454017.98328	2454436.02512	2455172.4183(13)
2454018.06257	2454436.10313	2455173.12604
2454018.14187	2454436.18234	2455204.3636(13)

Note. [a] $\sigma = 0.00045$ day except those given in parentheses.

in Figure 4 of Zhou & Liu (2003). The error for maximum determination is normally around 0.00045 day or less. The maxima are reported in Table 2. Those maxima followed by error bars in parentheses were adopted from Wils et al. (2009, 2010).

Before applying Fourier analysis for detecting pulsation contents, we have carefully dealt with the mean magnitude of light curves for different data sets, i.e., zero points in Fourier analysis. Because our CCD aperture photometry used non-uniform comparison stars and all the light-curve data are uncalibrated differential magnitudes obtained using several instruments, light curves on different nights may not be on the same mean level. Direct subtraction of nightly means may have a problem especially for a short light curve. Therefore, we have aligned data sets for each season individually by putting all those data in the range determined by the best night's data (template night) for that season. We shift every other night's data relative to the template night until we see they are in the same range and on the same level. The aligning is processed by trial and error and is monitored graphically. Close attention was paid to those light curves which do not cover a full pulsation cycle. The means of the resulting data sets for each season were then subtracted so as to merge them together.

In addition, we would like to check if there is an effect caused by the adjacent faint star (GSC 01739−01964) on the target. Thus whenever GP And is separated from its faint companion, aperture photometry is performed for GP And itself only. However, the faint star at most times cannot be resolved from the variable. We could measure GP And's brightness alone only for several hours on three nights in 2008 January obtained

by the 2.16 m telescope. We compared these data with others and found no obvious differences, so we conclude that we can ignore any effects on our pulsation analysis due to inclusion of the faint companion.

3. DATA ANALYSIS

Our aim is to characterize the pulsations of GP And from its light variations. Attempts are given below to resolve low-amplitude pulsations and to examine variability in pulsation amplitude and period. Hence, besides our data, we considered existing data from the literature: the measurements in 1975 (792 in the V band and 813 in the B band) by Gieseking et al. (1979) and the 189 V magnitudes from Szeidl et al. (2006). The combination of all V data is called data set "1975–09."

3.1. O−C Analysis

We analyzed the observed times of maximum light minus the calculated ones, i.e., the so-called $(O − C)$ residuals, to detect secular period change. The maxima of GP And's light curves have been recently compiled by Szeidl et al. (2006), who collected 131 maxima. Apart from that collection, a few more maxima were found in the literature. These sources are three maxima at HJD 2454031.840, 2454034.830 and 2453680.34246 from the AAVSO database and another one at HJD 2453680.35518(31) from Klingenberg et al. (2006). We found that the four maxima at HJD 2442258.5290, 2442289.4520, 2442289.5300, and 2442630.5421 from Rodríguez et al. (1993) and the one at 2433861.4380 (Eggen 1978) were not used by Szeidl et al. (2006). In addition, we have eight maxima at HJD 2441710.2470, 2442255.4710, 2442272.5430, 2442280.5410, 2442365.3080, 2442403.2300, 2442709.6186, and 2442711.6622 from earlier unpublished data. Ten maxima were obtained by Wils et al. (2009, 2010). Together with our 78 new maxima (see Table 2) we have a total of 238 maxima at our disposal.

To calculate the $(O − C)$ residual from maximum light timing and its corresponding cycle (denoted by E below) elapsed since an initial epoch, we have adopted the revised ephemeris HJD$_{max}$ = 2441909.49167 + 0.078682737 E given by Rodríguez et al. (1993). A quick view on the $(O−C)$ residuals shows that several timings of maximum light yield large $(O−C)$ scatter. We discarded 12 outlying points corresponding to the maxima: 2443861.438 (by Eggen 1978), 2441710.2470, 2442255.4710, 2442272.5430, 2442280.5410, 2442365.3080, 2450438.4732, 2451768.5280, 2451882.4580, 2453680.3415, 2454031.8400, and 2454034.8300. The last three maxima (from AAVSO) appear to be less accurate: one was directly determined from unfiltered observations without correction, and the other two were determined by fitting to just a few data points.

As a linear fit did not account for the distribution of the $(O − C)$ residuals as shown by previous researchers, we applied a second-order polynomial least-squares fit to the remaining 226 $(O − C)$ residuals and we got

$$HJD_{max} = 2441909.49177 + 0.078682698\,E$$
$$+ 4.65 \times 10^{-13}\,E^2 \qquad (1)$$

with a standard deviation of the fitting residuals of $\sigma = 0.00069$ day. Each data point was equally weighted in fitting. The quadratic coefficient indicates a positive rate of period change $\dot{P} \equiv dP/dt = 4.32 \times 10^{-9}$ days yr^{-1}. We also calculated the
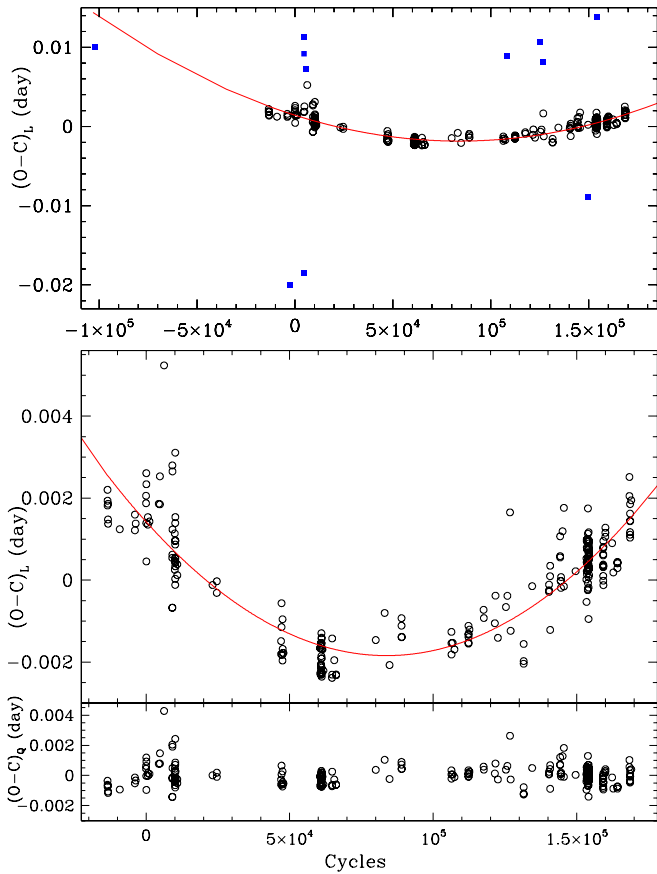
Figure 1. $O-C$ diagram for GP And. The solid curve is a quadratic fit based on 226 times of maximum light (in circles) without regard to the 12 maxima (in squares, top panel). The bottom panel shows the $(O-C)$ residuals of the fitting.

(A color version of this figure is available in the online journal.)

Figure 2. Amplitude spectra of GP And's light variations. Dashed vertical lines indicate the harmonics' positions. Solid curves refer to detection limit of $S/N = 4.0$.

(A color version of this figure is available in the online journal.)

commonly used measure $\dot{P}/P = (5.49 \pm 0.1) \times 10^{-8}$ yr^{-1}, which is comparable to that obtained by Szeidl et al. (2006) and to the theoretical prediction (Breger & Pamyatnykh 1998). This solution could correspond to continuous period changes caused by stellar evolution. A forced quadratic fit to all 238 maxima resulted in a worse fitting with $\sigma = 0.0026$ day. The fitting results along with the differences between the observed and the calculated times of maximum light are plotted versus the cumulative cycle numbers in Figure 1. In this $O-C$ diagram we also draw those maxima ignored in the above fitting. As seen, the first maximum by Eggen (1978) can be marginally fitted by the solution in Equation (1).

3.2. Pulsation Analysis

3.2.1. Fourier Analysis

To examine the multiperiodicity of GP And, we performed Fourier analyses for the entire data set "1975–09." Our approach was to remove the harmonics from the data, and then search for new frequencies in the residuals. This is a normal method for high-amplitude radial pulsators. It is sufficient to follow a statistical criterion to terminate the harmonic series. Generally, the amplitude of a signal at the detection limit level takes the role in deciding which terms to retain. Thus, we found that removing the first eight harmonics ($f_0 \sim 8f_0$) is sufficient.

The Fourier analyses were performed using PERIOD04 (Lenz & Breger 2005). The amplitude spectrum based on raw light curves for the 1975–09 data set along with the residuals
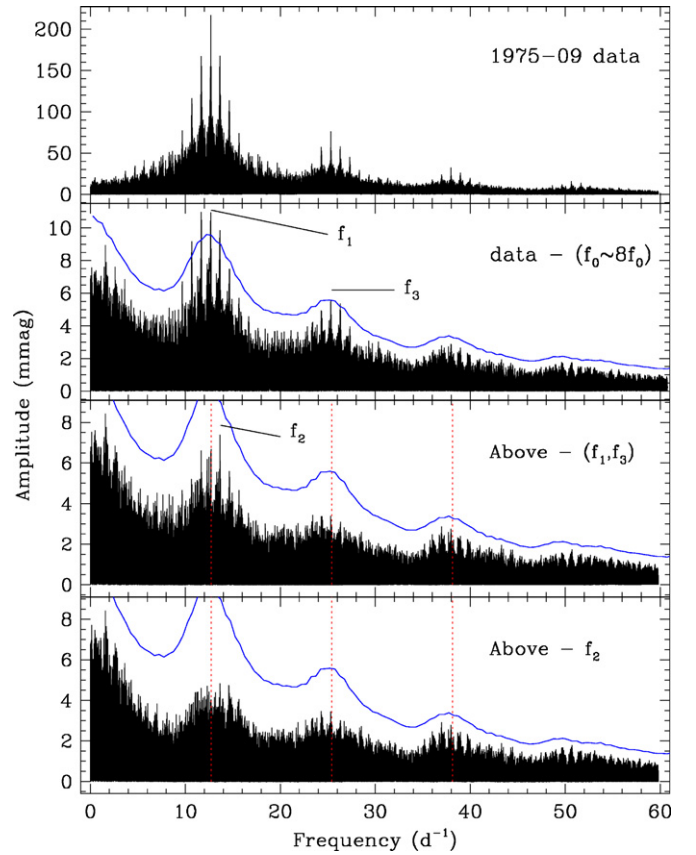
prewhitened by $f_0 \sim 8f_0$ harmonics are given in Figure 2. We have drawn the detection limit at a signal-to-noise ratio (S/N) of 4.0 in the residual spectra following the criterion by Breger et al. (1993) and Kuschnig et al. (1997). Signal is defined as the amplitude of the least-squares fit for a certain frequency, while the noise is taken as the average amplitude of the residuals in a frequency range of 3.0 day^{-1} (34.71 μHz) that encloses the detected peak. The residuals were computed from the original measurements with the first eight harmonics prewhitened.

As seen in Figure 2, the residuals in the second panel (counted from top) are not random noise. The marked peak $f_1 \sim$ 12.71 day^{-1} is outstanding. Another peak at $f_3 \sim 25.42$ day^{-1} is marginally significant (S/N = 4.3). After removing f_1 and f_3, the residual spectrum in the third panel leaves an additional peak at $f_2 \sim 13.69$ day^{-1} (S/N = 3.7), which is accompanied by symmetrical daily-aliased sidelobes. After further prewhitening f_2, the final residual spectrum drawn in the bottom panel shows a random white noise distribution.

These three peaks have lower amplitudes and could be significant only if the detection limit were overestimated. However, f_1 and f_2 are closely spaced to the main frequency f_0 and f_3 is near the harmonic $2f_0$. They are also correlated with each other by $(f_1 + f_2) - f_3 = 0.98226$, $f_2 - f_1 = 0.97859$, and $f_3 - 2f_1 = 0.00367$. Frequency f_3 may be the harmonic of f_1, while f_1 and f_2 are likely caused by aliasing. Since the main pulsation frequency f_0 is itself variable, it would not have been accurately removed from the original light curves when prewhitening. This incomplete prewhitening would result in some lower amplitude peaks near f_0 in the residuals. Below

4

Table 3
Comparison of the Frequency Analyses Among Different Subsets of Data

Item	Data Sets					
	1975–2009	2006–2009	2006–2007	2006–2007	2007	2006
Points	13558	10707	7402	7402	1799	5604
Nights	50	35	28	28	5	23
Interval (days)	12464.87	1198.95	466.93	466.93	5.19	71.94
Length (days)	7.723	5.867	5.084	5.084	1.248	3.836
Length (hr)	185.3	140.8	122.0	122.0	30.0	92.1
Δf (day^{-1})	8.0E-5	8.3E-4	0.002	0.002	0.19	0.014
$\Delta f'$ (day^{-1})	0.020	0.028	0.036	0.036	0.24	0.043
f_0	12.709261	12.709252	12.709254	12.70915[4]	12.70921	12.70922
Aliasing peaks						
f_1	12.71125	12.72822	12.73046	12.71022[4]	–	–
f_2	13.68984	13.69809	13.69758	13.71895[4]	–	13.69579
f_3	25.41883	–	25.80845	25.41938[4]	–	–

Notes. A dash refers to null detection.
[a] By CLEAN algorithm.

we will check the validity of these three suspected peaks. We will prove that they are not intrinsic pulsation frequencies but result from unresolved aliasing.

3.2.2. Checking for Alias Frequencies

Here we examine the validity of the three suspected peaks visible from the whole data set's residual spectrum in Figure 2. First, we applied the same Fourier analysis to the four subsets of the 1975–2009 data: 2006–2009, 2006–2007, 2007, and 2006. Then we compared the above results of the 1975–2009 data with those of the four subsets. Special attention was paid to the best subset "2006–2007." We show its Fourier spectrum in Figure 3, where $f_1 \sim 12.730$, $f_2 \sim 13.697$, and $f_3 \sim 25.808$ day^{-1} are visible below the significance curve. After prewhitening f_1 there is no outstanding peaks in the residual spectra. In addition, by using the CLEAN algorithm (Roberts et al. 1987), we got three peaks for the 2006–2007 data with amplitudes over 0.006 mag around f_0 and $2f_0$. The comparison is summarized in Table 3, where the trial peaks were picked up according to their S/N values (>3.7). We give the frequency resolution calculated not only from the time span (correspondingly Δf) but also from the number of actual days having data (correspondingly $\Delta f'$). The latter value $\Delta f'$ would pose a rigorous restrict on a peak closely spaced to a known frequency.

We see that peaks f_1 and f_2 appeared in three data sets 1975–2009, 2006–2007, and 2006–2009, while f_3 is visible in two data sets 1975–2009 and 2006–2007. Only f_2 was detected in the longest single year data set (2006). One reason could be that the 2006 data set's frequency resolution is too low to resolve the other two peaks.

It is known that a spectral window[3] describes the overall aliasing effect involved in data. We show aliasing patterns for our combined data set 1975–2009 at several scales in Figure 4. We are now able to inspect the trial peaks with the data's various aliases. For convenience, let us label the strongest aliases in Figure 4 as $g_0 = 0.00265$ day^{-1}, near the sidereal yearly alias of 0.0027378 day^{-1} (corresponding to 365.256363 solar days); $g_1 = 1.00265$ day^{-1}, near the sidereal daily alias of 1.0027379 day^{-1} (corresponding to 0.99726957 solar days or

---

[3] The Fourier spectrum of a window function, which is a single sine wave of arbitrary, but constant amplitude sampled at the same times as the data. It shows the aliasing pattern of the data.
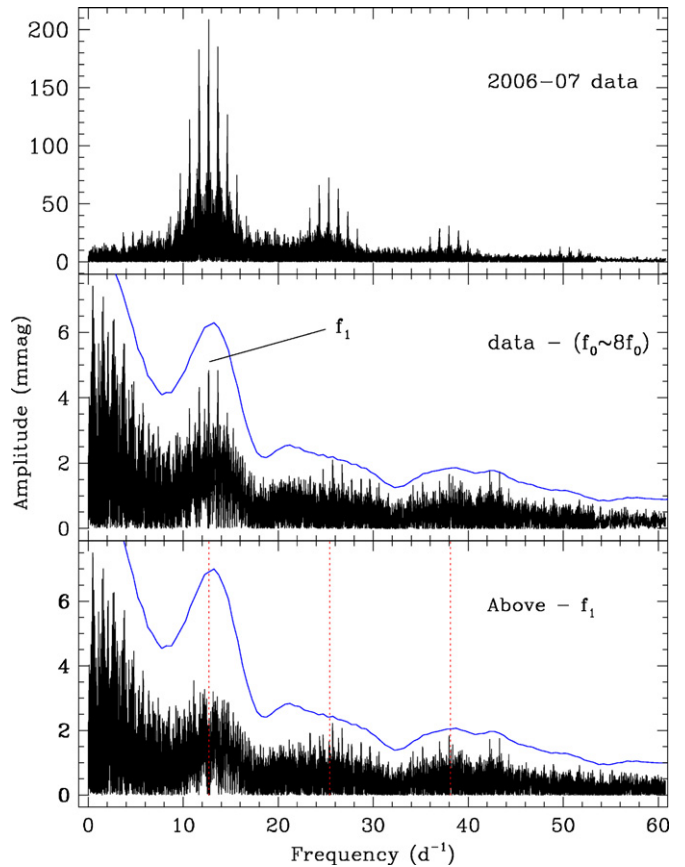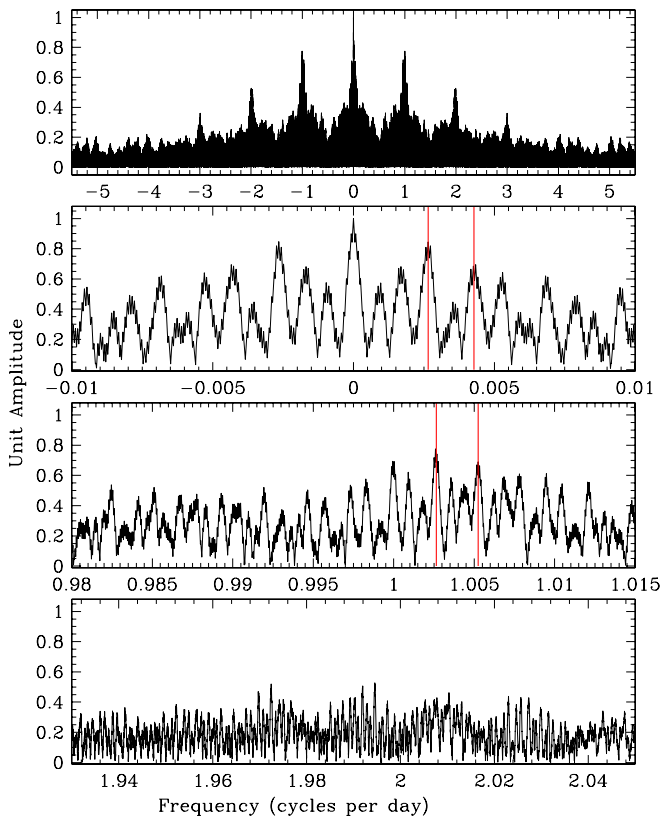

Figure 3. Same as Figure 2, but for 2006–2007 data.
(A color version of this figure is available in the online journal.)

$23^{\mathrm{h}}56^{\mathrm{m}}4\overset{s}{.}09$). For the 1975–2009 data set, we calculated that $f_1 - f_0 = 0.001989 = g_0 - 0.00066$; $f_2 - f_0 = 0.980579 = g_1 - 0.02207$; $f_3 - 2f_0 = 0.000308$. Besides daily gaps, there are several other data gaps between observing runs: 2493.93, 1360.96, 2591.37, 318.7448, 692.3119, 22.0519, 389.7908, 53.1149, and 485.6286 days. These gaps might yield aliases at 0.0004, 0.000735, 0.000386, 0.003137, 0.001444, 0.045347, 0.002565, 0.018827, and 0.002059 day^{-1}, respectively. Using $\Delta f' = 0.020$, f_1 and f_3 are most likely unresolved aliases of f_0 and $2f_0$, respectively.

Figure 4. Spectral window of the 1975–2009 data. The enlarged view panels show aliasing structure around 0, 1, and 2 day^{-1}. The labeled strongest aliases are 0.00265, 0.00428, 1.00265, and 1.00525 ± 0.00003 day^{-1}.

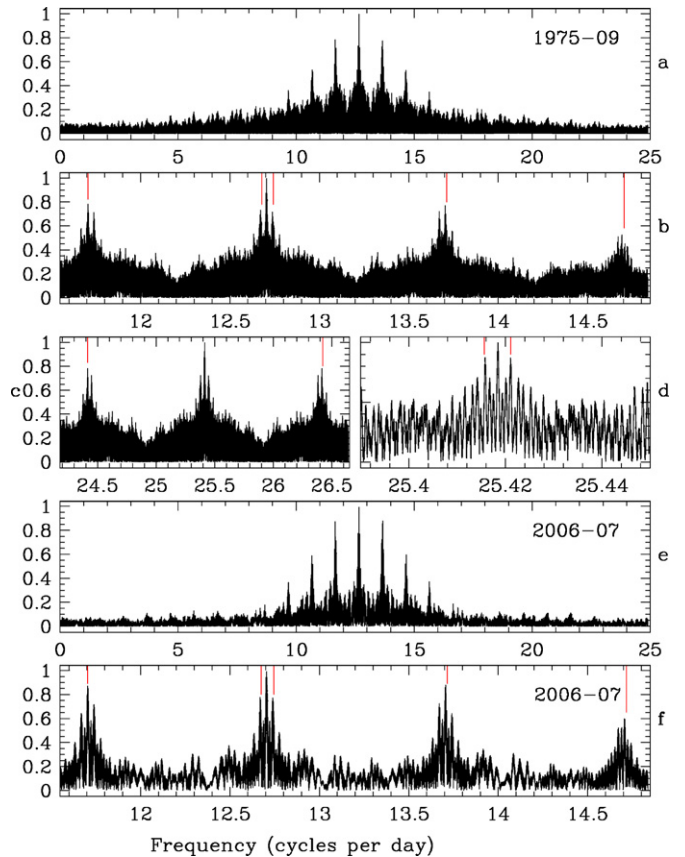(A color version of this figure is available in the online journal.)

Figure 5. Spectral windows centered at the input frequencies constructed by simulated light curves. Panels (a) and (e): actual aliasing pattern centered at f_0 for 1975–2009 and 2006–2007, respectively. The strongest aliases indicated in the enlarged-view panels are (b) 11.70666, 12.67828, 12.74228, 13.71185, 14.70381 day^{-1}; (c) and (d) aliasing pattern centered at $2f_0$: 24.41592, 26.42113, 25.41585, 25.42137 day^{-1}; (f) 11.70428, 12.67428, 12.74628, 13.71419, 14.71682 day^{-1}.

(A color version of this figure is available in the online journal.)

Similarly, for the 2006–2007 data set, we determined the following aliases: $g_0 = 0.0024$, $g_1 = 1.00258$, $g_2 = 2.0076 \pm 0.00006$ day^{-1}, and their interaction terms $2g_0$, $3g_0$, $g_0 + g_1$, $g_1 + 2g_0$, $g_2 + g_0$. Then we have for the Fourier results: $f_1 - f_0 = 0.021206$, $f_2 - f_0 = 0.988326 = g_1 - 0.01425$, $f_3 - 2f_0 = 0.38994$. Considering $\Delta f' = 0.036$, f_2 is an alias of f_0, but f_1 and f_3 cannot be explained as aliases. While for the CLEAN results, we have $f_1 - f_0 = 0.00107$, $f_2 - f_0 = 1.0098 = 1.0073$(alias)$+g_0+0.0001$, and $f_3 - 2f_0 = 0.00108$. We can therefore justify claiming all these peaks to be aliases.

Instead of producing a normal spectral window by taking the actual times of the observational data, t_i, we created artificial light curves of a single frequency with unit amplitude using the formula mag(t_i) = $0.0002 + 1.0 \sin[2\pi(\omega(t_i - T_0) + \phi)]$ (refers to Equation (2)). The Fourier transform of the artificial light curves exactly produces the inherent spectral window (i.e., aliasing pattern) of the raw light curves centered at frequency ω. In this manner, all other peaks except the input frequency ω are aliases. For $\omega = f_0$ and $2f_0$, $T_0 = 2442708.3566$, $\phi = 0.25$ we created such artificial light curves for the times of the 1975–2009 data set, while for $\omega = f_0$, $T_0 = 2454436.02512$, $\phi = 0.25$ we created artificial light curves for the times of the 2006–2007 data set. The results are displayed in Figure 5 and clearly indicates the alias frequencies presented in Figure 2.

Taking the various aliases, amplitudes, S/N values, and actual frequency resolution into consideration, we can safely conclude that f_1 and f_2 are alias peaks unresolved from f_0, while f_3 is an alias peak unresolved from $2f_0$ or harmonic of the alias of f_1.

3.2.3. Final Frequency Solution

As shown above, no new pulsations were identified, so GP And is a purely monoperiodic radial pulsator. Nonlinear least-squares fitting to the whole light curve with the harmonics $f_0 \sim 8f_0$ refined the fundamental frequency to be $f_0 = 12.7092609 \pm 0.0000002$ day^{-1} with semi-amplitude of 0.21453 ± 0.00023 mag. The fit resulted in a standard deviation of $\sigma = 0.0206$ minutes and zero point of $Z = 0.00139$ minutes.

Assuming mag(t) is the magnitude observed at time t, the fitting formula used for the light curves has the form

$$\mathrm{mag}(t) = Z + \sum_{i=1}^{n} A_i \sin[2\pi(\omega_i t + \phi_i)]. \tag{2}$$

Table 4 reports the Fourier coefficients obtained from the above fit. The analytical errors on the Fourier parameters including frequencies, amplitudes, and phases of the best-fitting sinusoids, were computed via the analysis program PERIOD04 which adopts the formulae derived by both Breger et al. (1999) and Montgomery & O'Donoghue (1999). For safety, we have assumed the residuals from the fit to be the rms deviations of observational noise corresponding to the data set. We usually adopt values at three times the calculated uncertainties, i.e., 3σ for the error bars of frequency and amplitude to be consistent with their practical errors and to avoid an underestimate by

Table 4
Results of Our Frequency Analysis of GP And Based upon All Available *V*-band Data in 1975–2009

Label	Frequency (ω_i, day^{-1})	Amplitude (A_i, mmag)	Phase (ϕ_i, 0–1)	Epoch (HJD)	S/N
f_0	12.7092609 ± 0.0000002	219.86 ± 0.23	0.7914 ± .0001	2454435.9515	92.1
$2f_0$	25.418522 ± 0.000004	80.65 ± 0.23	0.1830 ± .0005	2454435.9862	57.7
$3f_0$	38.127784 ± 0.000001	29.23 ± 0.23	0.9918 ± .0013	2454435.9975	35.8
$4f_0$	50.837045 ± 0.000002	13.16 ± 0.23	0.3763 ± .0028	2454436.0026	26.4
$5f_0$	63.546304 ± 0.000005	6.48 ± 0.23	0.8755 ± .0057	2454436.0057	16.3
$6f_0$	76.255561 ± 0.000008	3.93 ± 0.23	0.8742 ± .0094	2454436.0206	14.3
$7f_0$	88.964832 ± 0.000012	2.39 ± 0.23	0.9453 ± .0152	2454436.0203	8.8
$8f_0$	101.674076 ± 0.000021	1.35 ± 0.23	0.2979 ± .0266	2454436.0202	7.9

Note. Error bars with values of 3σ are adopted.

fitting theory. Except for the error for f_0 being much smaller than the frequency resolution, which could be attributed to its high amplitude, other errors are comparable with the frequency resolution. In this table, the epochs corresponding to phases ϕ_i of frequency ω_i are calculated relative to the initial epoch $T_0 = $ HJD 2454436.02512 (one of the observed timings of maximum brightness, at which phase is assumed to be 0.25) by

$$\text{Epoch}(\phi_i) = T_0 - (\text{fraction}[T_0 * \omega_i + \phi_i] + 0.25)/\omega_i. \quad (3)$$

The new differential light curves along with the fit containing sine curves of frequencies $f_0 \sim 8f_0$ and three aliasing contents $f_1 \sim f_3$ are presented in Figure 6.

3.3. Amplitude Variability

3.3.1. Cycle-to-cycle Amplitude Variations

Peak-to-peak amplitudes (PPAs) of individual pulsation cycles are variable from cycle to cycle for many high-amplitude pulsators. Autocorrelation analysis is a simple method for looking for cyclic behavior in variable star data. This method is able to detect characteristic timescales averaged over all the data. It is excellent for stars with amplitude variations and/or transient periods. We used ASTROLAB (Percy 2001) to perform self-correlation analysis for our best data set 2006–2007. In this method, for all pairs of measurements, the difference in magnitude (ΔV in a number of bins) and the difference in time (time lag, τ) to an upper limit are calculated. This limit was set to be a few times greater than the expected timescales (i.e., period). Then ΔV is plotted against τ in Figure 7, where the height of the maxima is a measure of the average pulsation amplitude of the variability, so this graph shows clear cycle-to-cycle amplitude variations. The average ΔV is a minimum at multiples of τ. Each minimum corresponds to the characteristic cyclic light variations timescales, i.e., pulsation period 0.0786828 ± 0.0000001 days (or frequency $f_0 = 12.7092609 \pm 0.0000002$ day^{-1}). The height of the minima was actually determined by the average error of the magnitudes and by the degree of irregularity. If the variability were perfectly periodic and the magnitudes had no error, then the minima would fall to zero. One can see that the higher the minimum, the larger the τ is.

3.3.2. Annual-scale Amplitude Variations

The Fourier amplitudes, which are the amplitudes of constant-frequency sinusoidal waves, are the mean values in the time period under investigation. In order to investigate longer timescale variability in pulsation amplitude, we have performed nonlinear least-squares fits to each subset of the data individually.

We fit the light curves with the fundamental frequency $f_0 = 12.709261$ day^{-1} and its harmonics fixed but allowing the amplitudes and phases to vary. We draw the readers' attention to both the amplitudes of the fundamental frequency itself and that of all eight harmonics. Unsurprisingly, they showed more or less the same trend: since the year 2003 the pulsation amplitudes have decreased. The results are presented in Figure 8. Even though the determined amplitude errors may be higher than the analytic errors (denoted as σ), we have adopted the values of 3σ. As seen in Figure 8, the adopted error bars are invisible for our new data. We have ignored the presence of the three aliases from Section 3.2.2. Even if the three aliases were included in fitting, their amplitudes are less than that for $4f_0 - 8f_0$, and only 11% of the amplitude of f_0 (= 24.73/219.86), or 7% of the total amplitudes of $f_0 - 8f_0$ (= 24.73/357.05). So the three alias frequencies cannot change the behavior of amplitude variability for the main pulsation.

3.3.3. Search for a Pattern Indicative of Amplitude Modulation

Amplitude variability could be caused by a periodic modulation. An indication of modulated light variations is a pattern of two equally spaced frequencies around the intrinsic pulsation frequency—a triplet. Assuming that the amplitude of an intrinsic pulsation with frequency f_c was modulated slowly by a periodic modulating signal of frequency f_m, then we can describe the modulated light variation (with time t) as

$$A(1 + \beta \sin f_m t) \cos(f_c t), \quad (4)$$

where A is amplitude, β is called modulation index. This modulation would result in three frequency components at $f_c - f_m, f_c,$ and $f_c + f_m$. We know that f_c could be the fundamental frequency f_0 and its harmonics, i.e., $f_c = k f_0$ ($k = 1,2,3,\ldots$), as that observed in Blazhko[4] RRab stars—a type of single fundamental mode oscillator (Jurcsik et al. 2009). If we assume there were amplitude modulations superposed on the intrinsic pulsation of GP And then we would search for the above triplet pattern.

A zoom-in view of the vicinity of f_0, a check on the residual spectra prewhitened by the $f_0 \sim 8f_0$ components and their alias peaks (see the bottom panels of Figures 2 and 3), did not reveal any frequency triplet patterns. This is true for f_0 and the higher-order harmonics. Therefore, periodic amplitude modulation was not detected in the light variations of GP And.

---

[4] The Blazhko effect: the phenomenon of amplitude and phase modulation. Russian astronomer Sergey N. Blazhko first reported in the star RW Draconis. A Blazhko variable has light curves that are modulated on timescales of typically tens to hundreds of days.
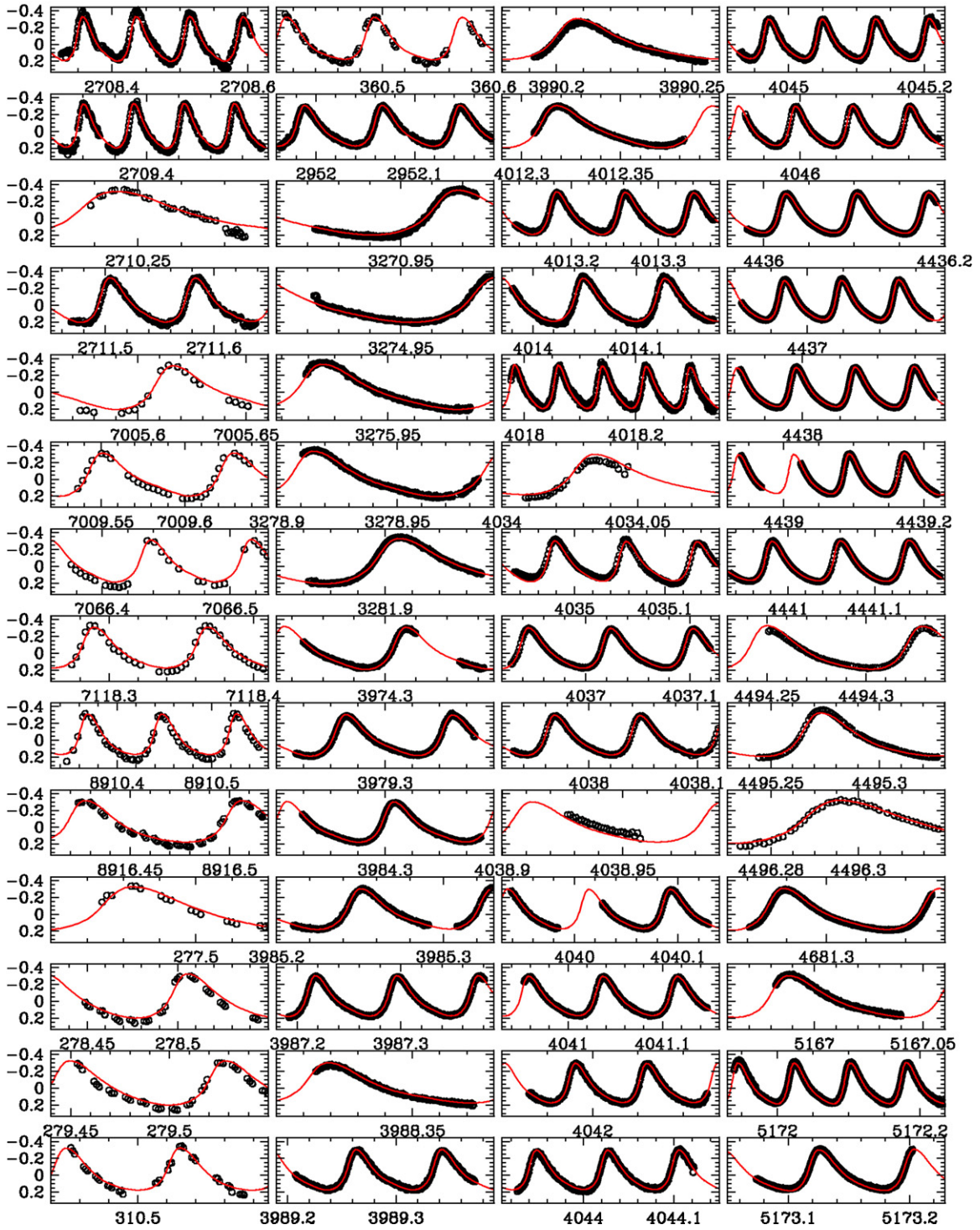
Figure 6. Entire *V*-band light curves (open circles) of GP And overplotted with the analytic curves involving sinusoids of the harmonics $f_0 \sim 8 f_0$ and aliases $f_1 \sim f_3$. For better printing, abscissa is given in modified HJD (2450000+ days, except panels 1–10 of the most left column in HJD 2440000+).

(A color version of this figure is available in the online journal.)

3.3.4. Re-examining Previous Claims of Amplitude Modulation

One reason for studying GP And was the previously reported amplitude modulation, which could vary from 0.6 to 0.7 minutes with a period of about 0.64 days (Gieseking et al. 1979). The authors had used PPAs of each pulsation cycle to derive this period. We tried to find this period in their data, so we redrew their light curves and measured the PPA values for both *V*

and *B* filters corresponding to each maximum epoch relative to their preceding minimum level. In the same manner, PPA values for our best data set 2006–2007 are also measured. The phase diagrams using the 0.64 day period and zero phase at the first maximum of each data set are drawn in Figure 9. Even though the shape looks periodic in the top panel for 1975 *V* data, it was not periodic in the bottom panel for the 2006–2007 data. Consequently, the 0.64 day periodic amplitude
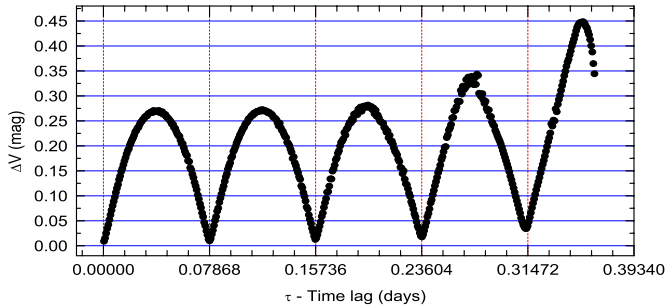
Figure 7. Cycle-to-cycle amplitude variations viewed by autocorrelation analysis for data set 2006–2007.

(A color version of this figure is available in the online journal.)

modulation is not verified for our 2006–2007 data. We attribute the claimed periodic modulation to misinterpretation of a few measurements.

4. DISCUSSIONS

4.1. Long-term Period Variability

Evolutionary models predict that the vast majority Population I HADS should show increasing periods, which are a factor of about ten times smaller than observed (Breger & Pamyatnykh 1998). Therefore, if the observed period changes of HADS are known sufficiently well, they can constrain theoretical calculations. The $O-C$ analysis for GP And leads us to the conclusion that the fundamental pulsation period of GP And was slowly increasing at a rate more or less matching the predictions of standard stellar evolutionary models.

4.2. Amplitude Variability

According to Breger (2000), for all cases of amplitude variability in δ Sct stars, their origin is presently not yet understood. Rodríguez (1999) performed a detailed analysis of the behavior of pulsation amplitude for seven monoperiodic HADS and concluded that long-term changes of amplitude of the light curves for any of the sampled stars are not significant. However, our investigation for GP And shows that its pulsation amplitude exhibited evident variations over time. Amplitude variability of HADS deserves extensive investigations.

4.3. The Frequency Solution

Although combining different observing seasons' data improved the frequency resolution in Fourier analysis, it also brought about complicated aliases. Due to frequency variability, prewhitening is incomplete and leaves confusing low-amplitude peaks close to the known frequencies. By creating artificial light curves, we could produce exactly the actual aliasing patterns in the data, revealing three suspected frequency peaks f_1, f_2, and f_3 to be artifacts. Thus, the pulsation frequency solution of GP And is simple. After removing the eight harmonics as well as the three aliasing frequencies, the residuals shown in the last panel of Figure 2 are generally random noise. Figure 6 looks like a perfect fit. However, a close view demonstrated in Figure 10 shows that a deviation between the observations and fit around extrema cannot be neglected. What has caused the deviation—cycle-to-cycle amplitude variability or an incomplete frequency solution? Further intensive high time resolution photometry like that obtained in 2007 may help in probing this phenomenon.
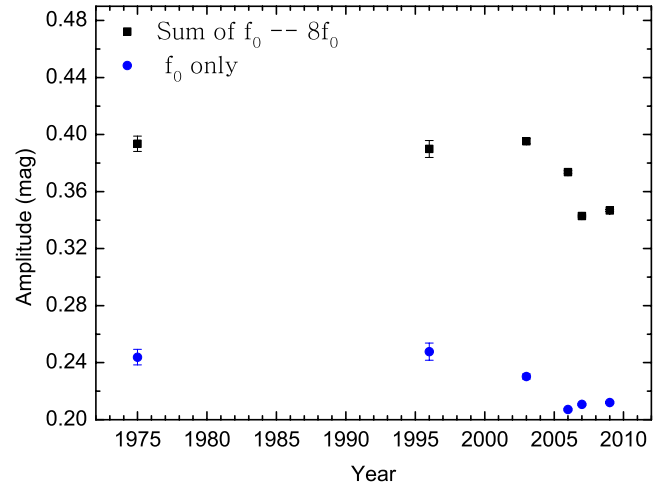

Figure 8. Annual mean pulsational amplitudes of GP And as a function of time.

(A color version of this figure is available in the online journal.)

4.4. Nonradial Modes and Multi-periodicities

We are particularly interested in resolving nonradial pulsations or multiple radial modes in known high-amplitude pulsators. We have devoted efforts to analyzing the light variations of an HADS, GP And, toward detecting nonradial modes. Unfortunately, we failed. Nevertheless, future efforts will be diverted to other high-amplitude pulsators. We would like to add our arguments to such efforts here.

Nonradial pulsations in classical high-amplitude pulsators, which were previously believed to have only one or multiple radial modes, have been increasingly reported in recent years (see an early review by Kovács 2002). Such pulsators are characterized by the presence of two or more frequencies very closely spaced to the known radial modes.

Olech et al. (1999) are probably the first astronomers who reported the presence of nonradial modes in three RRc stars (first overtone pulsators) of the globular cluster M55. Moskalik (2000) found nonradial modes in 11 RRab (fundamental-mode) pulsators from 149 samples and in two RRc from 66 samples in the Galactic Bulge. Alcock et al. (2000) presented an exciting discovery of RRc variables with closely spaced frequencies, which cannot be explained without invoking nonradial pulsation components. AQ Leo was the first known double-mode RR Lyrae pulsator (RRd star, with first overtone and fundamental radial modes). Three decades after its discovery (by Jerzykiewicz & Wenzel 1977), MOST[5] observations have revealed that AQ Leo oscillated with at least 42 frequencies, of which 32 are linear combinations (up to the sixth order) of the radial fundamental mode and its first overtone. The other intrinsic frequencies may represent an additional nonradial pulsation mode and its combination peaks with the two dominant radial modes (Gruberbauer et al. 2007).

A systematic search for multiperiodic pulsations in RR Lyr-type stars of the globular cluster ω Centauri had been conducted by Moskalik & Olech (2008), who had detected nonradial secondary periodicities close to the primary pulsation frequency in 17 out of 70 studied RRab and in 31 out of 81 RRc. They argued that in these newly detected periodicities, beating with the primary radial pulsation leads to a slow amplitude and phase

---

[5] MOST: Microvariability & Oscillations of STars, a Canadian space mission launched on 2003 June 30, which is a microsatellite housing a 15 cm Maksntov telescope feeding a CCD photometer through a single custom broadband filter in 350–700 nm.
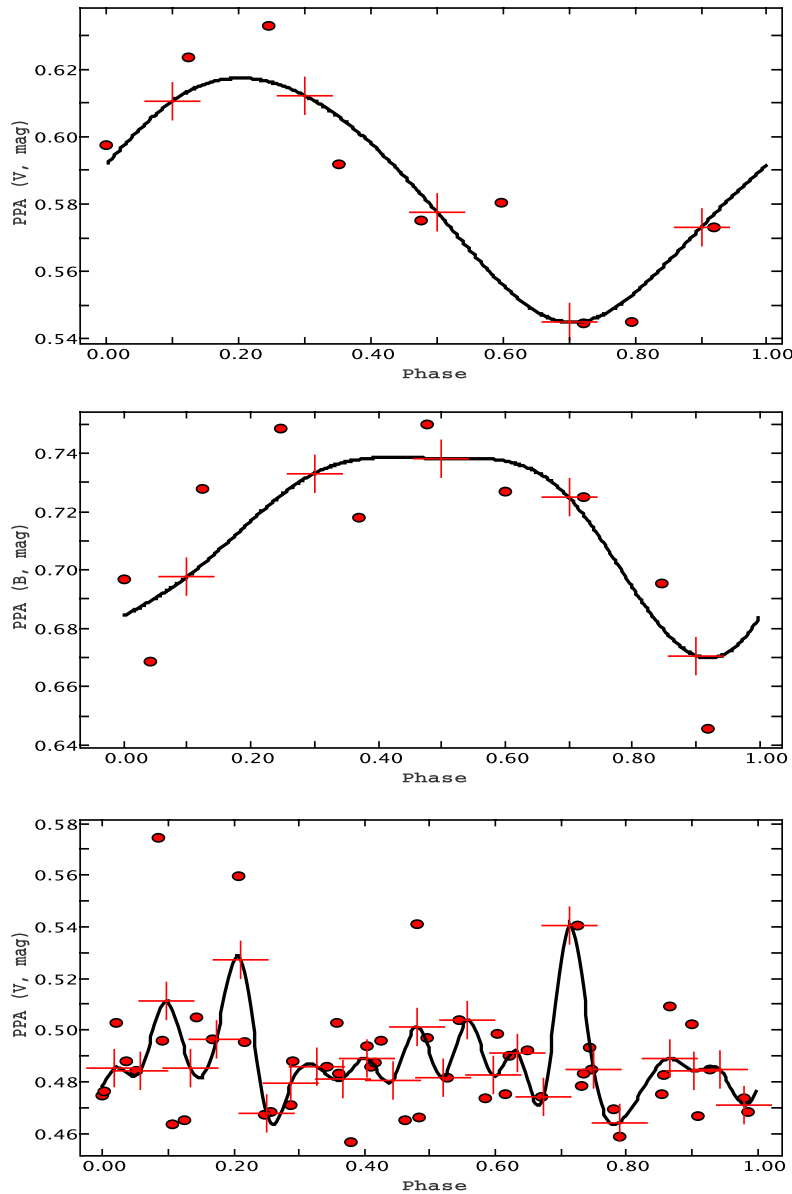
Figure 9. Examination of the 0.64 day periodic amplitude modulation. Solid curves are smooth connection of binned phases (in crosses). Top: 1975 *V*-filter data; middle: 1975 B data; bottom: 2006–2007 *V* data.

(A color version of this figure is available in the online journal.)

modulation, commonly referred to as the Blazhko effect. It is commonly understood that resonance and magnetic models explaining the Blazhko effect, both involve nonradial pulsation components (Kovács 2009). If that is true, Blazhko RR stars are actually mixed radial and nonradial pulsators.

More results can be found from the ASAS,[6] MACHO,[7] and OGLE[8] projects. Amplitude and phase modulation in RR Lyr

stars were also reported by CoRoT[9] (e.g., Szabó et al. 2009). The first results on RR Lyr stars from the Kepler mission[10] revealed the "period doubling" phenomenon caused by resonances of two pulsation modes, for the first time in RR Lyr, V808 Cyg, and V355 Lyr (Kolenberg et al. 2010). The period doubling phenomenon shows apparent variation at twice the actual period in the light curves. These authors found that a significant fraction of RRab stars show the Blazhko modulation. Period doubling may lead astronomers to unveil the mystery of the Blazhko effect (Szabó et al. 2010).

---

[6] The All Sky Automated Survey (ASAS) project is located at Las Campanas Observatory in Chile. Its main goal is to monitor the whole available bright sky (8 mag< *V* <14 mag) and search for variability. One of its main objectives is to find and catalog variable stars.

[7] The MACHO Project is a collaboration between scientists at the Mt. Stromlo & Siding Spring Observatories, the Center for Particle Astrophysics of the University of California, and the Lawrence Livermore National Laboratory. Its primary aim is to test the hypothesis that a significant fraction of the dark matter in the halo of the Milky Way is made up of objects like brown dwarfs or planets: these objects have come to be known as MACHOs, for MAssive Compact Halo Objects (refer to http://wwwmacho.mcmaster.ca/)

[8] The Optical Gravitational Lensing Experimental (OGLE; Udalski et al. 1992) is devoted to search for dark matter in our galaxy through the detection of microlensing events.

[9] Launched on 2006 December 27, the COROT (COnvection, ROtation & planetary Transits) space telescope (27 cm diameter) is a mission of astronomy led by CNES in association with French laboratories (CNRS) and with several international partners. Asteroseismology and search for exoplanets are its two main scientific objectives. See http://smsc.cnes.fr/COROT/.

[10] NASA's first mission capable of finding Earth-size planets around other stars. Launched on 2009 March 6, 0.95 m aperture photometer with detectors of 95 mega pixels (21 modules each with two 2200×1024 pixel CCDs) on a primary mirror of 1.4 m diameter. Refer to http://kepler.nasa.gov/.
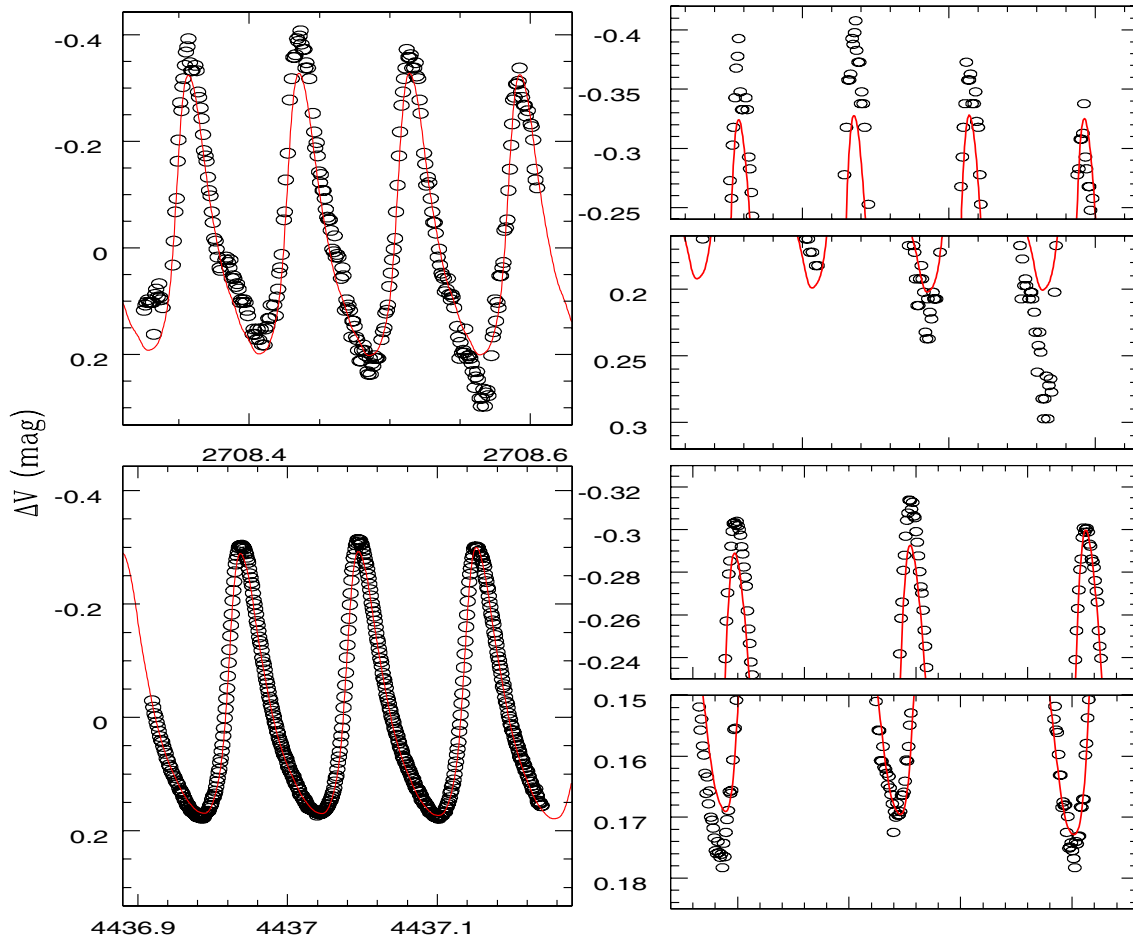
Figure 10. Close view on the 11 frequency fit. The right-hand panels are the zoomed-in view for the portions around extrema of the left light curves, on HJD 2442708.3–2708.6 night (1975, upper left) and on HJD 2454436.9–4437.2 night (2007 December 2, lower left), respectively.

(A color version of this figure is available in the online journal.)

Multiple radial-pulsation periods (more than two) are actually rare among high-amplitude pulsators. Currently there are four pulsating stars with three radial modes in our Galaxy: the classical Cepheids (DCEP, Population I) AC And (Fitch & Szeidl 1976) and V823 Cas (Antipin 1997), together with the δ Sct stars V829 Aql (Handler et al. 1998) and GSC 0762-0110 (Wils et al. 2008), which are pulsating in the fundamental, first, and second overtone modes. Recently, five such triple-mode DCEP pulsators were identified in the Large Magellanic Cloud (LMC): two of them are similar to the Galactic ones, but the other three are pulsating in the first, second, and third overtone modes (Soszyński et al. 2008). Moskalik et al. (2004) and Moskalik & Kołaczkowski (2008, 2009) reported the detection of low-amplitude periodicities in a few DCEPs of the LMC. These newly discovered periodicities were interpreted as nonradial modes.

Motivated by the above findings, Mulet-Marquis et al. (2007) investigated nonradial oscillations in classical Cepheids. However, nonradial pulsation in Cepheids involves a problem that has not been theoretically revised since the work of Dziembowski (1977) and Osaki (1977). The problem is that theoretical excitation of nonradial modes only occurs for rather high spherical harmonics with $\ell \geqslant 6$, while those with lower-order spherical harmonics are stable.

SX Phoenicis-type (SXPHE) is a subgroup of high-amplitude pulsators, which have high space velocities and fall into the blue straggler domain of the color–magnitude diagrams of globular clusters which characteristically are metal-deficient old, Population II stars. The periods of the SXPHE stars are shorter ($\sim 0\overset{d}{.}035$–$0\overset{d}{.}075$) than the HADS (Nemec & Mateo 1990; McNamara 1997, and references therein). The prototype SX Phe itself (Rolland et al. 1991) and the field SXPHE star BL Cam (Rodríguez et al. 2007) are identified to be multiperiodic radial and nonradial pulsators.

HADS are distinct from the RRab, RRc, RRd, DCEP, and SXPHE stars mentioned above in several respects: they are Population I, metal-rich, young, and in the Galactic field. The number of known HADS with multimode oscillations has gradually increased recently, hinting at a new potential for the asteroseismic studies of these objects (Poretti 2003; Poretti et al. 2005). Some of the stars might have nonradial pulsation modes present (McNamara 2000; Poretti et al. 2005). Examples have been added to this class in the last decades, that were previously thought to be mono-periodic or double-mode pure radial pulsators, but now are known to be pulsating with more radial and nonradial periods. Examples include AI Vel (the prototype of HADS; Walraven et al. 1992) and DY Peg (Garrido & Rodríguez 1996). Most recently, cycle-to-cycle radial velocity variations of AD CMi were observed, which might be due to nonradial pulsations (Derekas et al. 2009). Derekas et al. also confirmed another HADS BQ Ind's multiperiodic nature.

As previously noted by Garrido & Rodríguez (1996), microvariability, at the millimagnitude level, is becoming a common phenomenon among HADS. They believe that the

Table 5
Multiperiodic High-amplitude Pulsating Variables With Nonradial-mode Pulsation (NRP)

Pulsators	Type	NRP	Remarks	Reference
AC And	DCEP	?	Galactic field; F, 1O, 2O triple modes	Fitch & Szeidl (1976)
V823 Cas	DCEP	?	Galactic field; F, 1O, 2O triple modes	Antipin (1997)
2+3	DCEP	?	In LMC, (F, 1O, 2O)+(1O, 2O, 3O) triple modes	Soszyński et al. (2008, 2010)
a few	DCEP	Yes	In LMC	Moskalik & Kołaczkowski (2009)
139	DCEP	Yes	Of 1644 1O in SMC, 7th part of OGLE-III CVS	Soszyński et al. (2010)
V829 Aql	DSCT	?	Galactic field; F, 1O, 2O triple modes	Handler et al. (1998)
GSC 0762-0110	DSCT	?	Galactic field; F, 1O, 2O triple modes	Wils et al. (2008)
AD CMi	HADS	Yes	RV varies	Derekas et al. (2009)
BQ Ind	HADS	Yes	NRP confirmation is needed	Derekas et al. (2009)
RY Lep	HADS	Yes	NRP confirmation is needed	Rodríguez et al. (2003)
DY Peg	HADS	Yes	NRP confirmation is needed	Garrido & Rodríguez (1996)
AI Vel	HADS	Yes	2 radial and 3 nonradial modes	Walraven et al. (1992)
35/150	RRab	Yes	Galactic Bulge, OGLE-I database	Moskalik & Poretti (2003)
73/1435	RRab	Yes	Galactic field, ASAS catalog	Szczygieł & Fabrycky (2007)
12.2%	RRab	Yes	In LMC, MACHO project	Alcock et al. (2003)
15%	RRab	Yes	Of 5455 in LMC, OGLE-II fields	Soszyński et al. (2003)
17/70	RRab	Yes	In ω Cen; nonradial secondary periodicities	Moskalik & Olech (2008)
3	RRc	Yes	In globular cluster M55	Olech et al. (1999)
3/65	RRc	Yes	Galactic Bulge, OGLE-I database	Moskalik & Poretti (2003)
49/756	RRc	Yes	Galactic field, ASAS catalog	Szczygieł & Fabrycky (2007)
60/1327	RRc	Yes	In LMC, MACHO project	Alcock et al. (2000)
9.6%	RRc	Yes	In LMC, MACHO data revisit	Nagy & Kovács (2006)
6%	RRc	Yes	Of 1655 in LMC, OGLE-II fields	Soszyński et al. (2003)
many	RRc,RRab	Yes	In LMC, 3rd part of OGLE-III CVS	Soszyński et al. (2009)
31/81	RRc	Yes	In ω Cen	Moskalik & Olech (2008)
23%	RRe	Yes	Of 272 in LMC, OGLE-II fields	Soszyński et al. (2003)
many/600+	RR	Yes	Galactic Bulge, in SMC, OGLE-II	Mizerski (2004)
BL Cam	SXPHE	Yes	Multiple nonradial modes	Rodríguez et al. (2007)
SX Phe	SXPHE	Yes	A couple of nonradial modes	Rolland et al. (1991)

Notes. Interesting potential candidates are notated by "?." NRP incidence rate in a sample and individual NRP stars are given in first column. RRab or RR0: single fundamental mode (F) RR Lyr stars; RRc or RR1: single first overtone (1O) RR Lyr stars; RRd or RR01: fundamental and first overtone modes RR Lyr stars; RRe or RR2: single second overtone (2O) RR Lyrae stars.

phenomenon is just detectable when high-quality observations are available and can be of considerable interest because it would impose tight constraints on theoretical models of stellar pulsation. The new frequency, whether a higher radial overtone or a nonradial mode, should produce nonlinear interaction terms with the radial high-amplitude ones, at the corresponding amplitude level. We think that the unprecedented number of frequencies detected with amplitudes down to millimagnitude precision in turn presents an opportunity to test nonlinear theories of mode growth. Although unveiling nonradial components in HADS is hard work, the potential to extend our knowledge of the internal structure of these stars challenges us to do it.

In this regard, observational implications of detecting nonradial pulsations in high-amplitude radial pulsators for theoretical models are self-evident. Table 5 summarizes several types of multiperiodic high-amplitude pulsating stars in the instability strip with currently confirmed or suspected nonradial pulsation. This is by no means a complete statistic covering all such pulsators, but it is an illustration which compels us to study nonradial pulsations of high-amplitude pulsators.

5. CONCLUSIONS

This study was aimed primarily at finding multiperiodic pulsations and periodic amplitude modulation in the HADS star GP And. On the basis of the largest set of photometric time-series data to date, which were collected from 1975 to 2009 with several different telescopes and instruments, we have investigated its pulsational properties more deeply

than before. However, no further pulsations were detected beyond the primary pulsation frequency and its harmonics. GP And is consequently a purely monoperiodic radial pulsator. Deviations between fits and observations occurred on some nights (see Figure 10). They could be attributed to short time scale amplitude variations at the cycle-to-cycle level. We found the pulsation amplitudes to vary over the course of our observations (Figure 8). However, periodic modulation as a cause of amplitude variability was not verified.

The secular pulsational behavior of GP And was thoroughly studied by means of $O-C$ analysis and Fourier transforms. Our $O-C$ analysis (Figure 1) found that GP And's period is slowly and continuously increasing at the rate of $\dot{P}/P = (5.49 \pm 0.1) \times 10^{-8}$ yr^{-1} which matches the predictions of standard stellar evolutionary models—the majority of δ Sct stars should have constant or increasing periods.

With the acquisition of more extensive, higher-precision CCD photometric observations and the release of variability sky surveys' data, especially those from space telescopes, detections of nonradial modes in previously known purely radial high-amplitude pulsators should increase. In this context, we have roughly reviewed the current status of multiperiodicity and nonradial pulsation features among the high-amplitude pulsators in the classic instability strip (see Table 5).

REFERENCES

Alcock, C., Allsman, R., Alves, D. R., et al. 2000, ApJ, 542, 257
Alcock, C., Alves, D. R., Becker, A., et al. 2003, ApJ, 598, 597
Antipin, S. 1997, A&A, 326, L1
Breger, M. 2000, MNRAS, 313, 129
Breger, M., Handler, G., Garrido, R., et al. 1999, A&A, 349, 225
Breger, M., Stich, J., Garrido, R., et al. 1993, A&A, 271, 482
Breger, M., & Pamyatnykh, A. A. 1998, A&A, 332, 958
Derekas, A., Kiss, L. L., Bedding, T. R., et al. 2009, MNRAS, 394, 995
Dziembowski, W. A. 1977, Acta Astron., 27, 95
Eggen, O. J. 1978, IBVS, 1517
Fitch, W. S., & Szeidl, B. 1976, ApJ, 203, 616
Garrido, R., & Rodríguez, E. 1996, MNRAS, 281, 696
Gieseking, F., Hoffmann, M., & Nelles, B. 1979, A&AS, 36, 457
Gruberbauer, M., Kolenberg, K., Rowe, J. F., et al. 2007, MNRAS, 379, 1498
Handler, G., Pikall, H., & Diethelm, R. 1998, IBVS, 4549
Huang, L., Wu, H., & Li, H.-B. 2005, BFOSC (BAO Faint Object Spectrograph and Camera) Operating Manual (Beijing: BAO)
Jerzykiewicz, M., & Wenzel, W. 1977, Acta Astron., 27, 35
Jurcsik, J., Sódor, Á., Szeidl, B., et al. 2009, MNRAS, 400, 1006
Klingenberg, G., Dvorak, S. W., & Robertson, C. W. 2006, IBVS, 5701
Kolenberg, K., Szabó, R., Kurtz, D. W., et al. 2010, ApJ, 713, 198
Kovács, G. 2002, in ASP Conf. Ser. 259, Radial and Nonradial Pulsations as Probes of Stellar Physics, ed. C. Aerts & T. R. Bedding (San Francisco, CA: ASP), 396
Kovács, G. 2009, in AIP Conf. Proc. 1170, Stellar Pulsation: Challenges for Theory and Observation, ed. J. A. Guzik & P. A. Bradley (Melville, NY: AIP), 261
Kuschnig, R., Weiss, W. W., Gruber, R., Bely, P. Y., & Jenkner, H. 1997, A&A, 328, 544
Lenz, P., & Breger, M. 2005, Commun. Asteroseismol., 146, 53
McNamara, D. H. 1997, PASP, 109, 1221
McNamara, D. H. 2000, in ASP Conf. Ser. 210, Delta Scuti and Related Stars, ed. M. Breger & M. H. Montgomery (San Francisco, CA: ASP), 373
Mizerski, T. 2004, in ASP Conf. Ser. 310, Variable Stars in the Local Group, ed. D. W. Kurtz & K. R. Pollard (San Francisco, CA: ASP), 124
Montgomery, M. H., & O'Donoghue, D. 1999, Delta Scuti Star Newsletter, 13, 28
Morlet, G., Salaman, M., & Gili, R. 2000, A&AS, 145, 67
Moskalik, P. 2000, in ASP Conf. Ser. 203, The Impact of Large-Scale Surveys on Pulsating Star Research, ed. L. Szabados & D. W. Kurtz (San Francisco, CA: ASP), 315
Moskalik, P., & Kołaczkowski, Z. 2008, Commun. Asteroseismol., 157, 343
Moskalik, P., & Kołaczkowski, Z. 2009, MNRAS, 394, 1649
Moskalik, P., Kołaczkowski, Z., & Mizerski, T. 2004, in ASP Conf. Ser. 310, Variable Stars in the Local Group, ed. D. W. Kurtz & K. Pollard (San Francisco, CA: ASP), 498
Moskalik, P., & Olech, A. 2008, Commun. Asteroseismol., 157, 345
Moskalik, P., & Poretti, E. 2003, A&A, 398, 213
Mulet-Marquis, C, Glatzel, W., Baraffe, I., & Winisdoerffer, C. 2007, A&A, 465, 937
Nagy, A., & Kovács, G. 2006, A&A, 454, 257
Nemec, J., & Mateo, M. 1990, in ASP Conf. Ser. 11, Confrontation Between Stellar Pulsation and Evolution, ed. C. Cacciari & G. Clementini (San Francisco, CA: ASP), 64
Olech, A., Kałużny, J., Thompson, I. B., et al. 1999, AJ, 118, 442
Osaki, Y. 1977, PASJ, 29, 235
Percy, J. R. 2001, BAAS, 33, 849
Pop, A., Liteanu, V., & Moldovan, D. 2003, Ap&SS, 284, 1207
Poretti, E. 2003, A&A, 409, 1031
Poretti, E., Suàrez, J. C., Niarchos, P. G., et al. 2005, A&A, 440, 1097
Roberts, D. H., Lehar, J., & Dreher, J. W. 1987, AJ, 93, 968
Rodríguez, E. 1999, PASP, 111, 709
Rodríguez, E., Fauvaud, S., Farrell, J. A., et al. 2007, A&A, 471, 255
Rodríguez, E., López-González, M. J., & López de Coca, P. 2000, A&AS, 144, 469
Rodríguez, E., Laney, C. D., Amado, P. J., Lopez-Gonzalez, M. J., & Joner, M. 2003, in 25th IAU Meeting, Joint Discussion 12, Solar and Solar-Like Oscillations: Insights and Challenges for the Sun and Stars, 32
Rodríguez, E., Rolland, A., & López de Coca, P. 1993, A&AS, 101, 421
Rolland, A., Rodríguez, E., López de Coa, P., & García-Pelayo, J. M. 1991, A&AS, 91, 347
Soszyński, I., Poleski, R., Udalski, A., et al. 2008, Acta Astron., 58, 153
Soszyński, I., Poleski, R., Udalski, A., et al. 2010, Acta Astron., 60, 17
Soszyński, I., Udalski, A., Szymański, M., et al. 2003, Acta Astron., 53, 93
Soszyński, I., Udalski, A., Szymański, M. K., et al. 2009, Acta Astron., 59, 1
Szabó, R., Kolláth, Z., Molnár, L., et al. 2010, MNRAS, 409, 1244
Szabó, R., Paparó, M., Benkö, J. M., et al. 2009, in AIP Conf. Proc. 1170, Stellar Pulsation: Challenges for Theory and Observation, ed. J. A. Guzik & P. A. Bradley (Melville, NY: AIP), 291
Szczygieł, D. M., & Fabrycky, D. C. 2007, MNRAS, 377, 1263
Szeidl, B., Schnell, A., & Pócs, M. D. 2006, IBVS, 5718
Udalski, A., Szymański, M., Kałużny, J., Kubiak, M., & Mateo, M. 1992, Acta Astron., 42, 253
Walraven, Th., Walraven, J., & Balona, L. A. 1992, MNRAS, 254, 59
Wils, P., Hambsch, F.-J., Lampens, P., et al. 2010, IBVS, 5928
Wils, P., Kleidis, S., Hambsch, F.-J., et al. 2009, IBVS, 5878
Wils, P., Rozakis, I., Kleidis, S., Hambsch, F.-J., & Bernhard, K. 2008, A&A, 478, 865
Zhou, A.-Y., An, D., Eggen, J. R., et al. 2006, Ap&SS, 305, 29
Zhou, A.-Y., Jiang, X.-J., Zhang, Y.-P., & Wei, J.-Y. 2009, Res. Astron. Astrophys., 9, 349
Zhou, A.-Y., & Liu, Z.-L. 2003, AJ, 126, 2462